

# Thermoelectric three-terminal hopping transport through one-dimensional nanosystems

Jian-Hua Jiang,<sup>1</sup> Ora Entin-Wohlman,<sup>2</sup> and Yoseph Imry<sup>1</sup>

<sup>1</sup>*Department of Condensed Matter Physics, Weizmann Institute of Science, Rehovot 76100, Israel*

<sup>2</sup>*Department of Physics and the Ilse Katz Center for Meso- and Nano-Scale Science and Technology, Ben Gurion University, Beer Sheva 84105, Israel*

(Dated: January 24, 2012)

A two-site nanostructure (e.g. a “molecule”) bridging two conducting leads and connected to a phonon bath is considered. The two relevant levels closest to the Fermi energy are connected each to its lead. The leads have slightly different temperatures and chemical potentials and the nanostructure is also coupled to a thermal (third) phonon bath. The  $3 \times 3$  linear transport (“Onsager”) matrix is evaluated, along with the ensuing new figure of merit, and found to be very favorable for thermoelectric energy conversion.

PACS numbers: 84.60.Rb, 72.20.Pa, 72.20.Ee

## I. INTRODUCTION

In thermoelectric transport temperature differences can be converted to (or generated by) electric voltages. Such phenomena have already found several useful applications. Current research is motivated by the need for higher performance thermoelectrics as well as the pursuit of understanding of various relevant microscopic processes (especially the inelastic ones). Theory<sup>1–3</sup> predicts that high values of the thermopower follow when the carriers’ conductivity depends strongly on energy. Indeed, in bulk systems, the thermoelectric effects necessitate electron-hole asymmetry, which is often rather small. However, in nanosystems, such asymmetry can arise in individual samples in ensembles with electron-hole symmetry on average. Moreover, inelastic processes and interference effects may play nontrivial roles in thermoelectric transport.<sup>3</sup> It is known that the thermoelectric performance is governed by the dimensionless figure of merit  $ZT$ ,<sup>4</sup> where  $T$  is the common temperature of the system and  $Z = \sigma S^2 / (\kappa_e + \kappa_{ph})$ , with  $\sigma$  being the electrical conductivity,  $S$  the Seebeck coefficient, and  $\kappa_e$  and  $\kappa_{ph}$  the electronic and the phononic heat conductivities, respectively. Both  $\kappa_e$  and  $\kappa_{ph}$  can be smaller in nanosystems<sup>5</sup> than in bulk ones, opening a route for better thermoelectrics.

Mahan and Sofo<sup>6</sup> have argued that the best thermoelectric efficiency can be achieved in systems where i) the energy width of the main conducting channel is very narrow, and ii) the phonon thermal conductivity is as small as possible. It was suggested that ii) can be also realized in nanoscale composite structures where phonons are scattered by large variations in geometry and abundant interfaces,<sup>7,8</sup> while i) leads<sup>6</sup> to a very small  $\kappa_e / (S^2 \sigma)$ , as indeed has been confirmed in studies of quantum dot arrays.<sup>9</sup>

Here we consider three-terminal thermoelectric transport in small one-dimensional (1D) nanosystems accomplished via inelastic phonon-assisted hopping, and show that such processes lead to several nontrivial proper-

ties. Although thermal transport properties of mesoscopic structures have been studied in the past,<sup>2,3,10,11</sup> investigations of three-terminal thermoelectric transport are just at their infancy.<sup>12</sup> Our main conclusions are drawn from the simple, but important, two localized-state junction in which hopping is *nearest-neighbor*.<sup>13</sup> Later, we briefly discuss larger 1D systems, which exhibit rather surprising features of the thermoelectric transport. We show that such systems may have a high figure of merit, as  $\kappa_e$  can become extremely small, while the thermopower,  $S$ , remains finite. Some of the thermoelectric transport coefficients we find correspond to transferring electric/thermal current via temperature difference between the electron system and a suitable phonon bath. Hopefully, such systems can be achieved within current technology and be useful in applications.

There are several related ideas in the literature. Reference 14 presented an early, ingenious, way to cool a finite 2D electron gas (which plays the role of the thermal bath) at low temperatures by elastic electron transitions to/from the leads. All the energies involved are only of order  $k_B T$ . Reference 15 provided an experimental realization of some of the suggestions of Ref. 14, with further analysis. Reference 16 demonstrated a quantum ratchet, converting the nonequilibrium noise of a nearby quantum point contact to dc current. Reference 17 suggested a sophisticated Carbon nanotube structure, designed to extract energy from a discrete local oscillator at ultralow temperatures. The present work considers the full three-terminal case, where the energies involved can be larger than  $k_B T$ , and a real reservoir can be cooled, not just one or several degrees of freedom.

## II. MODEL SYSTEM

### A. Hamiltonian

The Hamiltonian,  $H = H_e + H_{e-ph} + H_{ph}$ , consists of the electronic and phononic parts and the electron-

phonon interaction. The electronic part is (electronic operators are denoted by  $c$  and  $c^\dagger$ )

$$H_e = \sum_i E_i c_i^\dagger c_i + \sum_{k(p)} \epsilon_{k(p)} c_{k(p)}^\dagger c_{k(p)} + \left( \sum_{i,k(p)} J_{i,k(p)} c_i^\dagger c_{k(p)} + \sum_i J_{i,i+1} c_i^\dagger c_{i+1} + \text{H.c.} \right). \quad (1)$$

Here  $i$  labels the localized states, of energies  $E_i$  (including usual Coulomb-blockade effects; i.e., it is assumed implicitly that a large Hubbard interaction confines the occupation of each level to be 0 or 1) and  $k$  ( $p$ ) marks the extended states in the left (right) lead, of energies  $\epsilon_k$  ( $\epsilon_p$ ) (all energies are measured from the common chemical potential). The matrix element coupling the localized states to each other is  $J_{i,j}$ , and those coupling them to the lead states are  $J_{i,k(p)}$ . All are exponentially decaying, with a localization length  $\xi$ , e.g.,

$$J_{i,k(p)} = \alpha_e \exp\left(-\frac{|x_i - x_{L(R)}|}{\xi}\right), \quad (2)$$

with  $x_i$  and  $x_{L(R)}$  being the coordinates of the center of the localized states and the left (right) boundary, and the prefactor  $\alpha_e$  yielding the coupling energy. The electron-phonon interaction is

$$H_{e-ph} = \sum_{\mathbf{q}} M_{\mathbf{q},ij} c_i^\dagger c_j (a_{\mathbf{q}} + a_{-\mathbf{q}}^\dagger) + \text{H.c.}, \quad (3)$$

where the phonon modes, of wave vector  $\mathbf{q}$  and frequency  $\omega_{\mathbf{q}}$ , are described by the operators  $a_{\mathbf{q}}^\dagger$ ,  $a_{\mathbf{q}}$ . Their Hamiltonian is  $H_{ph} = \sum_{\mathbf{q}} \omega_{\mathbf{q}} a_{\mathbf{q}}^\dagger a_{\mathbf{q}}$  (we use units where  $\hbar = 1$ ). The electron-phonon coupling is  $M_{\mathbf{q},ij} = \alpha_{e-ph} \exp(-|x_i - x_j|/\xi)$ , with  $\alpha_{e-ph}$  being the electron-phonon coupling energy. The transport through the system is governed by hopping when the temperature is above a crossover temperature,  $T_x$ , estimated below in Sec. II C for the most important two-site case. At lower temperatures the dominant transport is via tunneling. The two-site example of our system is depicted in the upper panel of Fig. 1.

### B. Hopping and interface resistors

The system described above bridges two electronic leads, held at slightly different temperatures and chemical potentials,  $T_L$ ,  $\mu_L$ , and  $T_R$ ,  $\mu_R$ , such that the common temperature is  $T \equiv (T_L + T_R)/2$ . The golden-rule transition rate  $\Gamma_{ij}$ , between two localized states, located at  $x_i$  and  $x_j$  and having energies  $E_i < 0 < E_j$ ,<sup>18</sup> necessitates the inelastic electron-phonon scattering (3), and reads

$$\Gamma_{ij} = 2\pi \Gamma_{in} f_i (1 - f_j) N_B(E_{ji}), \quad (4)$$

where  $E_{ji} \equiv E_j - E_i$ , the carriers' local Fermi function is

$$f_i = \left[ \exp\left(\frac{E_i - \mu_i}{k_B T_i}\right) + 1 \right]^{-1}, \quad (5)$$

and  $N_B$  is the Bose function

$$N_B = \left[ \exp\left(\frac{\omega_{\mathbf{q}}}{k_B T_{ph}}\right) - 1 \right]^{-1}, \quad (6)$$

determined by  $T_{ph}$ , the temperature of the local phonon bath (see Fig. 1). We assume that this phonon bath is strongly coupled to a thermal reservoir and is thermally isolated as much as possible from the leads, such that its temperature is determined by that reservoir. On the other hand, phonons in the leads are in good thermal contact with the electrons there and share the same temperature. These assumptions are further elaborated upon in Sec. III C. In Eq. (4),  $\Gamma_{in} = |M_{\mathbf{q},ij}|^2 \nu_{ph}(|E_{ij}|)$ , where  $\nu_{ph}$  is the phonon density of states. The linear hopping conductance at long distances ( $|x_i - x_j| \equiv |x_{ij}| \gg \xi$ ) and high energies ( $|E_i|, |E_j| \gg k_B T$ ) of the bond  $ij$  is<sup>18</sup>

$$G_{ij} \sim \frac{e^2}{k_B T} |\alpha_{e-ph}|^2 \nu_{ph}(|E_{ij}|) \eta_{ij}^{-1}, \quad \eta_{ij} = \exp\left(\frac{2|x_{ij}|}{\xi}\right) \exp\left(\frac{|E_i| + |E_j| + |E_{ij}|}{2k_B T}\right). \quad (7)$$

As opposed to Eq. (4), the tunneling conduction from, say, site  $i$  to the left lead can be accomplished by elastic tunneling processes with a transition rate  $\Gamma_{iL} = \gamma_{iL} f_i [1 - f_L(E_i)]$ , where  $\gamma_{iL} = 2\pi |J_{ik}|^2 \nu_L(E_i)$  and  $f_L$  and  $\nu_L$  are the Fermi distribution and density of states of the left lead. The corresponding linear interface conductance is then  $G_{iL} \simeq e^2 |\alpha_e|^2 \nu_L(E_i) (k_B T)^{-1} \exp[-2|x_{iL}|/\xi - |E_i|/(k_B T)]$ . This conductance (and the interface conductance at the right lead) will be assumed to be much larger than the hopping conductance between the two localized states.

### C. The two-site case

The thermopower in the hopping regime has been discussed by Zvyagin.<sup>19</sup> The simplest example is that of a two-site system ( $i, j = 1, 2$ ) depicted in Fig. 1, which describes, e.g. a diatomic molecule<sup>13</sup> or a series-connected double quantum dot.<sup>9</sup> In such a case transport is accomplished by nearest-neighbor hopping. As site 1 (2) is in a good contact with left (right) lead, we may assume that the local chemical potential and temperature there are  $\mu_{L(R)}$  and  $T_{L(R)}$ . The transport is dominated by the hopping from 1 to 2 when the temperature is higher than  $T_x$ . This temperature is estimated from the requirement that the elastic tunneling conductance across the system,  $G_{tun}$ , is comparable to the hopping one. The former is given by the transmission  $\sum_{i=1,2} \Gamma_{iL}(E) \Gamma_{iR}(E) / [(E - E_i)^2 + (\Gamma_{iL}(E) + \Gamma_{iR}(E))^2/4]$ , where the tunneling rates are  $\Gamma_{iL(R)}(E) = 2\pi |J_{i,k(p)}|^2 \nu_{L(R)}(E)$ . Since site 1 (2) is coupled mostly to the left (right) lead, we use their perturbation-theory mixtures, governed by the small parameter  $J_{12}/E_{21}$ . At

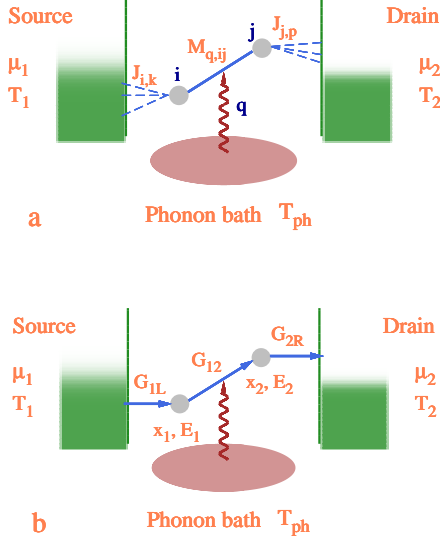


FIG. 1. (Color online) a. A two localized-state ( $i$  and  $j$ , gray points) system coupled to two leads, of temperatures  $T_L$  and  $T_R$ , and chemical potentials  $\mu_L$  and  $\mu_R$  (with the choice  $\mu_L > \mu_R$  and  $T_L > T_R$ ). The phonon bath temperature is  $T_{ph}$ . The localized states are coupled (dotted lines) to the continuum of states in the leads, and are also coupled (the wavy line) to the phonon bath; b. The effective resistors representing the system: The straight (blue) arrows indicate the net electronic currents and the wavy (brown) one the phonon heat current, with  $G_{1L}$ ,  $G_{2R}$ , and  $G_{12}$  being the conductances of the tunneling and the hopping resistors, respectively.

low temperatures and for  $|E_1|, |E_2| \gg \Gamma_1, \Gamma_2$ , where  $\Gamma_i \equiv \Gamma_{iL} + \Gamma_{iR}$ , we estimate

$$G_{tun} \sim e^2 E_1^{-2} |\alpha_e|^6 \nu_L(0) \nu_R(0) E_2^{-2} \exp\left(-\frac{2W}{\xi}\right), \quad (8)$$

where  $W$  is the system length between the leads. The hopping conductance is given by Eqs. (7) (with  $i, j = 1, 2$ ). Comparing those two, with exponential accuracy, the elastic tunneling mechanism can be important<sup>20</sup> only when

$$\exp\left[-\frac{|E_1| + |E_2| + |E_{12}|}{2k_B T}\right] \ll \exp\left[-2\frac{W - |x_{12}|}{\xi}\right] \\ \rightarrow \eta_{12} \gg \exp(2W/\xi), \quad (9)$$

giving  $k_B T_x \sim (|E_1| + |E_2| + |E_{12}|)\xi/[4(W - |x_{12}|)]$ .

### III. THREE-TERMINAL THERMOELECTRIC LINEAR TRANSPORT

#### A. Transport equations

The electronic particle current through the system is, as in Eq. (4) allowing for the temperature and chemical potential differences,

$$I_N = \Gamma_{12} - \Gamma_{21}. \quad (10)$$

For an electron transferred from left to right, the bath gives an energy  $-E_1$  ( $E_2$ ) to the left (right) lead, and thus the phonons transfer the energy  $E_{21}$  to the electrons. A net energy of  $\bar{E} \equiv [E_1 + E_2]/2$  is transferred from left to right. Hence, the net electronic energy current,  $I_Q^e$ , and the heat current<sup>21</sup> exchanged between the electrons and the phonons,  $I_Q^{pe}$ , are

$$I_Q^e = \bar{E} I_N, \quad \text{and} \quad I_Q^{pe} = E_{21} I_N. \quad (11)$$

The linear-response transport coefficients are obtained by expanding Eqs. (10) and (11) to first order in  $\delta T \equiv T_L - T_R$ ,  $\delta\mu \equiv \mu_L - \mu_R$ , and  $\Delta T \equiv T_{ph} - T$ ,

$$\begin{pmatrix} I_e \\ I_Q^e \\ I_Q^{pe} \end{pmatrix} = \begin{pmatrix} G & L_1 & L_2 \\ L_1 & K_e^0 & L_3 \\ L_2 & L_3 & K_{pe} \end{pmatrix} \begin{pmatrix} \delta\mu/e \\ \delta T/T \\ \Delta T/T \end{pmatrix}, \quad (12)$$

where  $I_e = eI_N$  is the charge current. All transport coefficients in Eq. (12) are given in terms of the linear hopping conductance  $G$  [given by Eqs. (7)],

$$L_1 = \frac{G}{e} \bar{E}, \quad L_2 = \frac{G}{e} E_{21}, \\ K_e^0 = \frac{G}{e^2} \bar{E}^2, \quad L_3 = \frac{G}{e^2} \bar{E} E_{21}, \quad K_{pe} = \frac{G}{e^2} E_{21}^2. \quad (13)$$

Note that  $L_2$ ,  $L_3$ , and  $K_{pe}$  are related to  $E_{21}$ , and  $I_Q^{pe}$  vanishes linearly with the latter.

The transport coefficients  $L_2$  ( $L_3$ ) correspond to, e.g., generating *electronic current* (*energy current*) via the temperature difference  $\Delta T$ .<sup>12</sup> When reversed, this process performs as a refrigerator: Electric current pumps heat current away from the phononic system and *cools it down*. In analogy with the usual two-terminal thermopower  $S$ , here we use the three-terminal thermopower<sup>12</sup> of this process,

$$S_p = \frac{L_2}{TG} = \frac{k_B}{e} \frac{E_{21}}{k_B T}. \quad (14)$$

Note that  $S_p$  of our model can be very large as the energy taken from the phonons per transferred electron can be several times  $k_B T$ .

#### B. Two-terminal figure of merit, for $\Delta T = 0$

A significant feature of our setup is that the electronic heat conductance can vanish while the thermopower stays finite

$$K_e = K_e^0 - \frac{L_1^2}{G} = 0, \quad S = \frac{L_1}{TG} = \frac{k_B}{e} \frac{\bar{E}}{k_B T}. \quad (15)$$

According to Ref. 6, the largest two-terminal figure of merit is achieved in systems with the smallest  $\kappa_e/\sigma S^2$  (provided that  $S$  stays finite). Here this ratio vanishes, and then  $Z$  is limited by  $\kappa_{ph}$ . The latter can be minute in

nanosystems.<sup>5</sup> Moreover, it can be reduced by manipulating phonon disorder and/or phonon-interface scattering (avoiding concomitantly drastic changes in the electronic system). Our system is then expected to possess a high figure of merit.

### C. Three-terminal figure of merit

The three-terminal geometry suggests novel possibilities for thermoelectric applications. For example, when  $\Delta T < 0$  and  $\delta\mu > 0$ , the setup serves as a refrigerator of the local phonon system, whose efficiency is given by the rate of the heat pumped from the phonon system to the electrical work invested,

$$\eta = I_Q^{pe} / (I_e \delta\mu) . \quad (16)$$

Consider first the special situation with  $\bar{E} = 0$ , where  $L_1 = K_e^0 = L_3 = 0$ . For a given  $\Delta T$ ,  $\delta\mu$  is adjusted to optimize the efficiency, yielding

$$\eta = \eta_0 (2 + \tilde{Z}T - 2\sqrt{\tilde{Z}T + 1}) / (\tilde{Z}T) , \quad (17)$$

where  $\eta_0 = T/|\Delta T|$  is the Carnot efficiency, and the new figure of merit is

$$\tilde{Z}T = L_2^2 / (GK_{pe} - L_2^2) . \quad (18)$$

Inserting here Eqs. (13) yields  $\tilde{Z}T \rightarrow \infty$  upon neglecting the “parasitic” conductances, discussed below. When  $\bar{E} \neq 0$ , such an optimization can be achieved by setting  $\delta T = 0$ .

In reality,  $\tilde{Z}T$  must be finite. To calculate a more realistic efficiency, we generalize Eq. (12) by adding the elastic transmission, the tunneling conductance  $G_{el}$ , to the hopping conductance  $G$ , and the elastic components,  $L_{1,el}$  and  $K_{e,el}^0$ , to  $L_1$  and  $K_e^0$ . (The elastic transmission does not contribute to  $L_2$ ,  $L_3$ , and  $K_{pe}$ , which are related to the heat transfer between the electronic and phononic systems.<sup>12</sup>) We also include the phonon heat conductance  $K_p$ , replacing  $I_Q^e$  by  $I_Q$ , the total heat current from the left to the right lead ( $\delta T$  is now also the temperature difference for the phononic systems in the left and right leads). Due to the absence of phonon-drag effects in localized electronic systems, the temperature difference  $\delta T$  should not contribute to other currents beside  $I_Q$ . Finally, there are phononic heat flows from the two leads to the system being cooled. Hence the numerator of Eq. (16) is replaced by  $I_Q^{pe} - K_{pp}\Delta T/T$ , where  $K_{pp}$  describes the phononic heat conductance in such processes.

Following the same procedure as above, the efficiency is optimized by adjusting  $\delta\mu$  at  $\delta T = 0$ . The result is similar, except that the figure of merit is modified,

$$\begin{aligned} \tilde{Z}T &= \frac{L_2^2}{(G + G_{el})(K_{pp} + K_{pe}) - L_2^2} \\ &= \left[ \frac{G_{el}}{G} + \frac{K_{pp}}{K_{pe}} + \frac{G_{el}K_{pp}}{GK_{pe}} \right]^{-1} . \end{aligned} \quad (19)$$

This has a straightforward physical interpretation: The wasted work is due to the elastic conductance and the unwanted heat diffusion, and  $\tilde{Z}T$  is limited by the ratio of the waste to the useful powers. In nanosystems  $K_{pp}$  can be limited by the contact between the system and the leads. Hence the ratios can be made small and  $\tilde{Z}T$  can still be *large*. The three-terminal device can also serve as a heater and as a thermoelectric battery, where the same figure of merit describes the efficiency.<sup>4</sup>

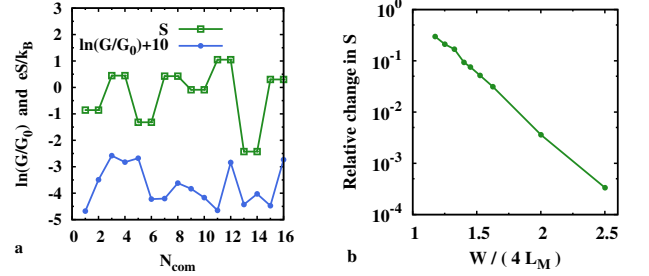


FIG. 2. (Color online) a. The conductance,  $\ln(G/G_0)$ , and thermopower,  $eS/k_B$ ; the abscissa gives the number of computations,  $N_{com}$ . The parameters are  $W = 800$ ,  $L_M = 20$ ,  $\xi = 3.3$ , in units average nearest-neighbor distance,  $T_0 = 3000$ ,  $T = 20$ , and the energy-band width is 1090 ( $T_0$  and  $L_M$  are the Mott<sup>19</sup> temperature and length, defined in the text). b. The relative change in  $S$  as a function of the system length  $W/(4L_M)$ , obtained by averaging over  $10^6$  random configurations. Parameters (except  $W$ ) are the same as in a.

### D. Longer 1D systems

For a chain of localized states, the picture is similar though slightly more complex. Consider first nearest-neighbor hopping, where the system is a chain of resistors. The same considerations as in the two-site case [in which the energy transferred is determined by site 1 (2) and the left (right) lead] hold here for the leftmost,  $\ell$ , (rightmost,  $r$ ) localized state and the left (right) lead. Hence, the thermoelectric transport is described by Eqs. (11)-(14), with  $E_1$  ( $E_2$ ) replaced by  $E_\ell$  ( $E_r$ ). In particular, the thermopower coefficients  $S$  and  $S_p$  are *completely determined* at the left and right *boundaries*, despite the fact that transport coefficients are usually determined by both the boundaries and the “bulk”.

In the variable-range hopping regime, the result is similar:  $S$  and  $S_p$  are determined by the resistors closed to the left and right boundaries, within a distance comparable to the Mott length. This observation is confirmed by numerical simulations. In Fig. 2a we plot the thermopower  $S$  and the conductance  $G$  for different random configurations in which the energies  $E_i$  and locations  $x_i$  of the sites are random: The  $E_i$  are chosen from a uniform distribution in the range  $[-E_{max}, E_{max}]$ , with  $E_{max} = 545$  (units are defined in the figure caption) being larger than the hopping energy,  $\sim (T_0 T)^{1/2}$ , determined by the Mott<sup>22</sup>

temperature  $T_0$  which is of the order of the level spacing on scale  $\xi$ ). The locations  $x_i$  are chosen from a uniform distribution in the range  $[0, W]$ , where  $W$  is the length of the sample in units of the nearest-neighbor distance. The conductance of the whole network is calculated by solving the Kirchhoff's equations,<sup>22</sup> which yields the currents through each bond for a given source-drain bias. The thermopower  $S$  is obtained from the particle current,  $I_N$ , and the heat current  $I_Q^e$  via the relation  $S = I_Q^e / (I_N e T)$ .

The heat current  $I_Q^e$  (particle current) is calculated by summing over the heat currents (particle currents) flowing through all the bonds *connected with the leads*. In each such bond ( $iL$ ) [ $iR$ ] which connects the  $i$ -th localized state to the left (right) lead, the heat current flow is  $I_Q^{(iL)} = E_i I_N^{(iL)}$  [ $I_Q^{(iR)} = E_i I_N^{(iR)}$ ] with  $I_N^{(iL)}$  [ $I_N^{(iR)}$ ] being the particle current in that bond. The total heat and particle currents are  $I_Q^e = 0.5 \sum_i (I_Q^{(iL)} + I_Q^{(iR)})$  and  $I_N = \sum_i I_N^{(iL)} = \sum_i I_N^{(iR)}$ , respectively.

At each  $N_{\text{com}}$ -th computation, with  $N_{\text{com}}$  being an odd number, a new random resistor network is generated. At the subsequent,  $N_{\text{com}} + 1$ -th, computation only the middle half part  $[W/4, 3W/4]$  of the network is replaced by a new random configuration, while the parts close to the left and right boundaries,  $[0, W/4]$  and  $[3W/4, W]$ , are *not* modified. It is seen from Fig. 2a that the conductance  $G$  changes dramatically when the central part is modified, whereas the thermopower is practically *immune to modifications of the central part*. To further study the sensitivity of the thermopower to the sites that are a distance larger than  $W/4$  away from the two interfaces as a function of  $W$ , we plot the relative change of the thermopower  $S$  as a function of  $W$  in Fig. 2b. This relative change is defined as  $|S_{2n+1} - S_{2n+2}| / |S_{2n+1} + S_{2n+2}|$ , where  $S_{2n+1}$  and  $S_{2n+2}$  denote the thermopowers calculated in the  $2n + 1$  and  $2n + 2$ -th computation, respectively. The results are obtained by averaging over  $10^6$  random configurations. It is seen that the relative change in  $S$  decays exponentially with increasing  $W$ , implying that sites located several Mott hopping distances  $L_M$  away from the boundaries have a negligible effect on the thermopower  $S$ . The Mott length,  $L_M$ , is of the or-

der of  $[\xi / (\nu k_B T)]^{1/(d+1)}$ , where  $\nu$  is the density of states at the Fermi level.

#### IV. SUMMARY AND CONCLUSIONS

In this work we studied the three-terminal thermoelectric transport and thermopower mainly in simple 1D hopping systems in the linear-response regime. We worked out the figure of merit for the three-terminal thermopower and expressed it as a function of the three-terminal thermoelectric transport coefficients. We obtained expressions for the thermoelectric transport coefficients in the simple two-site case. The system studied exhibits a large thermopower and high figure of merit in the appropriate cases. We analyze the conditions for high figure of merit in reality.

For longer 1D chains, we found that, contrary to intuition based on the usual conductances, the thermoelectric transport coefficients in hopping systems are *solely* determined by the states which are close to the interfaces (approximately, within the relevant hopping length). More details on these surprising results and their generalizations will be given elsewhere. Finally, it should be emphasized that *all* the results obtained here are in agreement with the systematic microscopic derivations which will appear in consequent work. Both Eq. (8) and Eq. (13) agree with the results derived from the non-equilibrium Green function method.

#### ACKNOWLEDGMENTS

We thank M. Pollak, A. Rosch, P. Wölfle and A. Amir for illuminating discussions. OEW acknowledges the support of the Albert Einstein Minerva Center for Theoretical Physics, Weizmann Institute of Science. This work was supported by the BMBF within the DIP program, BSF, by the ISF, and by its Converging Technologies Program.

- 
- <sup>1</sup> M. Cutler and N. F. Mott, Phys. Rev. **181**, 1336 (1969); N. F. Mott and E. A. Davis, *Electronic Processes in Non-crystalline Materials* (Clarendon, Oxford, 1979).
  - <sup>2</sup> U. Sivan and Y. Imry, Phys. Rev. B **33**, 551 (1986).
  - <sup>3</sup> C. W. J. Beenakker and A. A. M. Staring, Phys. Rev. B **46**, 9667 (1992).
  - <sup>4</sup> T. C. Harman and J. M. Honig, *Thermoelectric and thermomagnetic effects and applications* (McGraw-Hill, New-York, 1967); H. J. Goldsmid, *Introduction to Thermoelectricity* (Springer, Heidelberg, 2009).
  - <sup>5</sup> L. D. Hicks and M. S. Dresselhaus, Phys. Rev. B **47**, 12727 (1993); *ibid.*, 16631 (1993).

- <sup>6</sup> G. D. Mahan and J. O. Sofo, Proc. Natl. Acad. Sci. **93**, 7436 (1996).
- <sup>7</sup> M. S. Dresselhaus, G. Chen, M. Y. Tang, R. Yang, H. Lee, D. Wang, Z. Ren, J.-P. Fleurial, and P. Gogna, Adv. Mater. **19**, 1043 (2007).
- <sup>8</sup> R. Venkatasubramanian, Phys. Rev. B **61**, 3091 (2000); J.-K. Yu, S. Mitrovic, D. Tham, J. Varghese, and J. R. Heath, Nature Nanotech. **5**, 718 (2010).
- <sup>9</sup> T. E. Humphrey and H. Linke, Phys. Rev. Lett. **94**, 096601 (2005); N. Nakpathomkan, H. Q. Xu, and H. Linke, Phys. Rev. B **82**, 235428 (2010).
- <sup>10</sup> F. Giazotto, T. T. Heikkilä, A. Luukanen, A. M. Savin, and J. P. Pekola, Rev. Mod. Phys. **78**, 217 (2006).

- <sup>11</sup> M. Paulsson and S. Datta, Phys. Rev. B **67**, 241403 (2003).
- <sup>12</sup> O. Entin-Wohlman, Y. Imry, and A. Aharony, Phys. Rev. B **82**, 115314 (2010); R. Sánchez and M. Büttiker, Phys. Rev. B **83**, 085428 (2011).
- <sup>13</sup> The diatomic molecule case was experimentally investigated by, *e.g.*, O. Tal, M. Kiguchi, W. H. A. Thijssen, D. Djukic, C. Untiedt, R. H. M. Smit, and J. M. van Ruitenbeek, Phys. Rev. B **80**, 085427 (2009).
- <sup>14</sup> H. L. Edwards, Q. Niu, and A. L. de Lozanne, Appl. Phys. Lett. **63**, 1815 (1993); H. L. Edwards, Q. Niu, G. A. Georgakis, and A. L. de Lozanne, Phys. Rev. B **52**, 5714 (1995).
- <sup>15</sup> J. R. Prance, C. E. Smith, J. P. Griffiths, S. J. Chorley, D. Anderson, G. A. C. Jones, I. Farrer, and D. A. Ritchie, Phys. Rev. Lett. **102**, 146602 (2009).
- <sup>16</sup> V. Khrappai, S. Ludwig, J. P. Kotthaus, H. P. Tranitz, and W. Wegscheider, Phys. Rev. Lett. **97**, 176803 (2006).
- <sup>17</sup> S. Zippilli, G. Morigi, and A. Bachtold, Phys. Rev. Lett. **102**, 096804 (2009).
- <sup>18</sup> A. Miller and E. Abrahams, Phys. Rev. **120**, 745 (1960).
- <sup>19</sup> I. P. Zvyagin, Phys. Stat. Sol. (b) **58**, 443 (1973).
- <sup>20</sup> A treatment of tunneling vs hopping conductance is contained in A. D. Stone and P. A. Lee, Phys. Rev. Lett. **54**, 1196 (1985).
- <sup>21</sup> The heat taken from (delivered to) a reservoir with a chemical potential  $\mu$  by an electron with energy  $E$  leaving (entering) it is  $E - \mu$ , see J. M. Ziman, *Principles of The Theory of Solids* second edition, (Cambridge University Press, Cambridge, 1995), sections 7.7–7.9. We take the average  $\mu$  to be zero.
- <sup>22</sup> V. Ambegaokar, B. I. Halperin, and J. S. Langer, Phys. Rev. B **4**, 2612 (1971); H. Böttger and V. V. Bryksin, *Hopping Conduction in Solids* (Wiley-VCH, Weinheim, 1985); A. Amir, Y. Oreg, and Y. Imry, Phys. Rev. B **80**, 245214 (2009).